Numerical calculation of the VELO coupling impedance

N. van Bakel[a], J.F.J. van den Brand[a,b], M. Ferro-Luzzi[c]

[a] *Department of Physics and Astronomy, Vrije Universiteit, NL-1081 HV Amsterdam, The Netherlands*
[b] *National Institute for Nuclear Physics and High Energy Physics, NL-1009 DB Amsterdam, The Netherlands*
[c] *CERN, EP Division, CH-1211 Genève 23, Switzerland*

July 26, 2001

Abstract

We present simulation results obtained for the longitudinal impedance of the LHCb VELO detector corrugated encapsulation when the detector is in the 'closed' position. These results were obtained from time-domain calculations with the MAFIA package. The low frequency slope of the imaginary part of the longitudinal impedance is expected to be of the order of 5 mΩ.

LHCb note 2001-082 / VELO

1 Introduction

The LHCb vertex locator (VELO) [1] represents a major challenge in that it must provide identification and reconstruction of primary and secondary vertices with micrometer precision, at distances of a few millimeters from the interaction point (IP8). This is achieved by using a microstrip silicon tracker positioned at a distance of 8 mm from the beam axis, which corresponds to a full aperture (16 mm) smaller than that required by LHC during injection (minimum full aperture of 54 mm, see in Ref. [2]). As a consequence, the tracker must be retractable. To protect the LHC vacuum from excessive outgas rates due to various components of the detector modules, these are enclosed in a thin-walled container. The design of this encapsulation must also be optimized to minimize RF coupling to the beams, while taking into account degradation of the LHCb physics performance due to materials in the acceptance.

Various design solutions have been considered, starting from a design with one encapsulation per detector module [3]. Frequency-domain wake field calculations were carried out [4, 5] which showed that such a design would require the addition of thin shielding strips throughout the VELO setup, in order to avoid a dense spectrum of resonant frequencies with large shunt impedances. However, particle tracks in the LHCb experiment have low polar angles with respect to the beam axis. As a consequence, besides being a technically challenging solution, the use of long thin strips throughout the VELO setup considerably increases the amount of material traversed by particles. An alternative design was investigated, in which a single corrugated encapsulation is used for all modules of one detector half, as shown in Fig. 1 and 2. Frequency-domain wake field calculations were again performed and it was shown that such a design could be a viable solution, provided the corrugations are not too deep [6].

Apart from introducing high-frequency resonant modes and possible coherent effects, discontinuities in the structures surrounding the LHC beams also contribute to the total impedance of the storage ring. Longitudinal oscillations of the beam bunches can occur which are related to the low-frequency part of the longitudinal impedance. These oscillations, if too large and not compensated for, may induce unstable beam conditions. Because no longitudinal feedback will be used at the LHC, stringent limits are imposed on the longitudinal impedance budget [9]. It is therefore crucial to minimise the impedance of each component to be inserted in the ring. This applies as well for the LHCb VELO setup. Here, we continue our investigations on the RF properties of our baseline design solution by studying the low frequency behaviour of the longitudinal impedance.

2 Definitions

The quantity under study is the low-frequency slope of the imaginary part of the longitudinal impedance $Z_\parallel$. In many cases, the imaginary part of $Z_\parallel(\omega)$ decreases linearly with the frequency ω when $\omega \to 0$, while the real part vanishes more rapidly. One then writes $Z_\parallel(\omega) \simeq j\omega L + ...$, and

$$L = \frac{d\mathrm{Im}(Z_\parallel)}{d\omega}\Big|_{\omega=0} = \omega_{\mathrm{rev}}^{-1}\,\frac{d\mathrm{Im}(Z_\parallel)}{dn}\Big|_{n=0} \tag{1}$$

is called the 'inductance' of the device under study. Here, $n = \omega/\omega_{\mathrm{rev}}$ is the modal number, $\omega_{\mathrm{rev}} = 2\pi\nu_{\mathrm{rev}}$ and ν_{rev} is the revolution frequency ($\simeq 11245$ Hz for the LHC).

Simulation programs for time-domain wake field solutions (such as MAFIA's T3 solver [7] or ABCI [8]) usually yield the longitudinal wake potential $W_\parallel(s)$, where $s = vt - z$ is the longitudinal distance behind the bunch charge distribution $\rho(z)$, measured from the head of the distribution (see Fig. 3). The bunch moves in the positive z direction with speed v and t denotes time. The

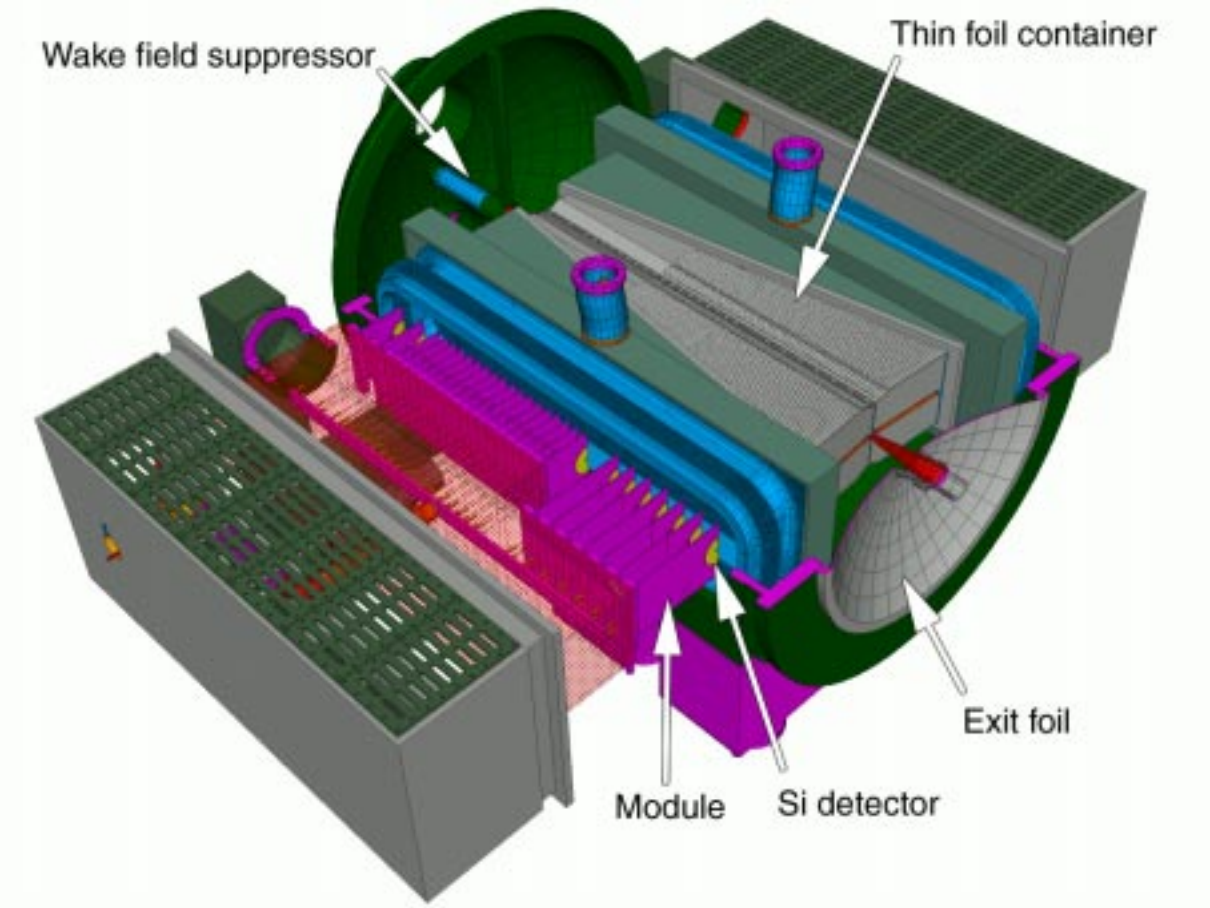

Figure 1: Three dimensional cut-out view of the VELO primary vacuum vessel, secondary vacuum containers and silicon detectors. One detector half is retracted from its vacuum container in order to show the silicon detector modules. The structure studied in this work is situated near the beam axis between the two thin-walled containers and is shown in Fig. 2.

longitudinal wake potential $W_\parallel(s)$ and impedance $Z_\parallel(\omega)$ are related by a Fourier transformation [10]. ABCI yields directly the real and imaginary parts of $Z_\parallel(\omega)$, in addition to $W_\parallel(s)$. For MAFIA, we use the C code `wtoz0.c` written by Scott Berg to Fourier-transform $W_\parallel$ and obtain $\mathrm{Re}(Z_\parallel)$ and $\mathrm{Im}(Z_\parallel)$.

For the charge distribution we use a gaussian-shaped bunch with length σ and which we cut off at $\pm 5\sigma$. The bunch moves with the speed of light $v = c$ and its head is positioned at the entrance of the modelled structure at time $t = 0$. The calculation is stopped at the earliest when the tail of the charge distribution is just outside the structure, *i.e.* at $t \geq (\ell + 10\sigma)/c$. We then extract the slope at $\nu = 0$ by a 1-parameter linear fit of $\mathrm{Im}(Z_\parallel)$ in the range $0 < \nu < 0.3$ GHz.

The VELO mechanical design to be investigated is shown in Fig. 1 and 2. The structures directly visible to the beams have no axial symmetry and exhibit geometrical changes (corrugations) with characteristic dimensions of the order of a few millimeters to a few centimeters. A full description of this setup in the MAFIA mesh generator would require excessive memory and CPU. However, for the case with the detector in the closed position, when the detector halves are spaced by about 1 mm, one can safely assume that the support structures and vacuum vessel surrounding the thin-walled encapsulations do not affect the beams. Hence, we model only the inner structures, shown in Fig. 2. Note that the detector slots of one half are staggered in the beam direction by half a corrugation to accomodate an overlap between detectors of opposite

halves. We started our simulations with a single 'cavity' (two detector slots on each half) and increased then the number of cavities ($N = 1...5$). In addition, for the case of a single cavity we repeated the calculations for different spaces between two subsequent detector slots. From these two studies we finally estimated the inductance for the whole corrugated structure.

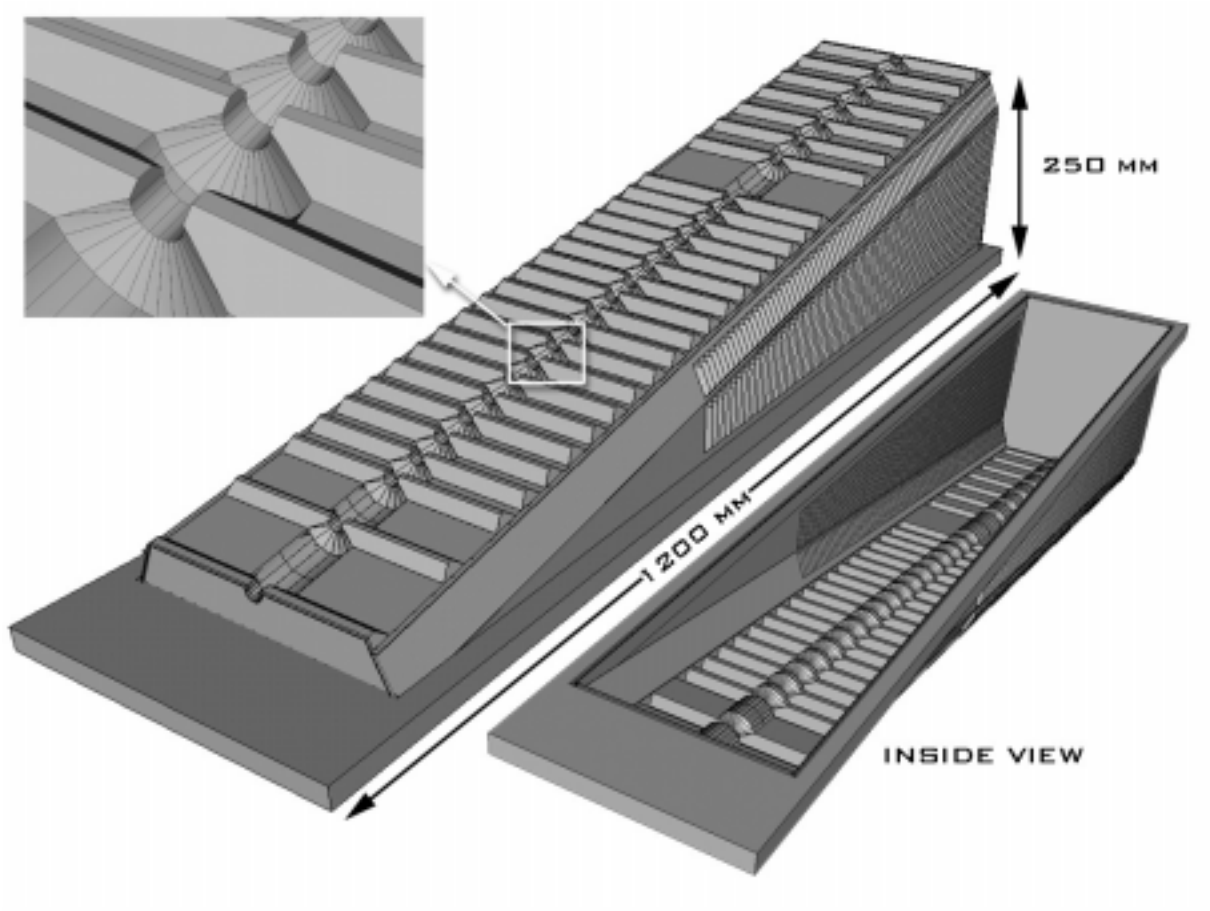

Figure 2: Three dimensional view of thin-walled encapsulation.

3 Checks with an axial-symmetric pillbox cavity

Since the calculated $W_{\parallel}(s)$ is defined on a discrete and finite mesh of s values, the accuracy of the resulting $Z_{\parallel}(\omega)$ depends on the mesh size used in the calculation and on the cut-off value $s_{\rm cut-off}$. Various checks were performed to verify that the mesh size and range of integration were adequate. In particular, we calculated the longitudinal wake potential $W_{\parallel}$ using ABCI for an axial symmetric pillbox of geometrical dimensions similar to the cavities present in our VELO setup. The pillbox model is shown in Fig. 3. For such a simple geometry the inductance can be estimated analytically. From Ref. [11] one expects

$$\frac{d{\rm Im}(Z_{\parallel})}{dn}\Big|_{n=0} = \omega_{\rm rev}\, L \simeq \omega_{\rm rev}\, \frac{\mu_0}{2\pi}\, \ell n(d/b)\, \frac{1-e^{-\gamma(\omega)g}}{\gamma(\omega)}\ , \tag{2}$$

where we have used $d = b + h$, $\gamma(\omega) = \sqrt{(\xi_0/d)^2 - (\omega/c)^2)}$, with $\xi_0 \simeq 2.4$ the first root of the Bessel function J_0, and c the speed of light. At low frequencies, with $a = 5$ mm, $b = 6$ mm, $g = 20$ mm and $h = 19$ mm, this expression gives

$$\frac{d{\rm Im}(Z_{\parallel})}{dn}\Big|_{n=0} \simeq \omega_{\rm rev}\, \frac{\mu_0}{2\pi\, \xi_0}\, \ell n(d/b)\, d\, (1-e^{-\xi_0 g/d}) \simeq 0.18\ {\rm m}\Omega\ . \tag{3}$$

Equivalently, the expected inductance is $L \simeq 2.54$ nH .

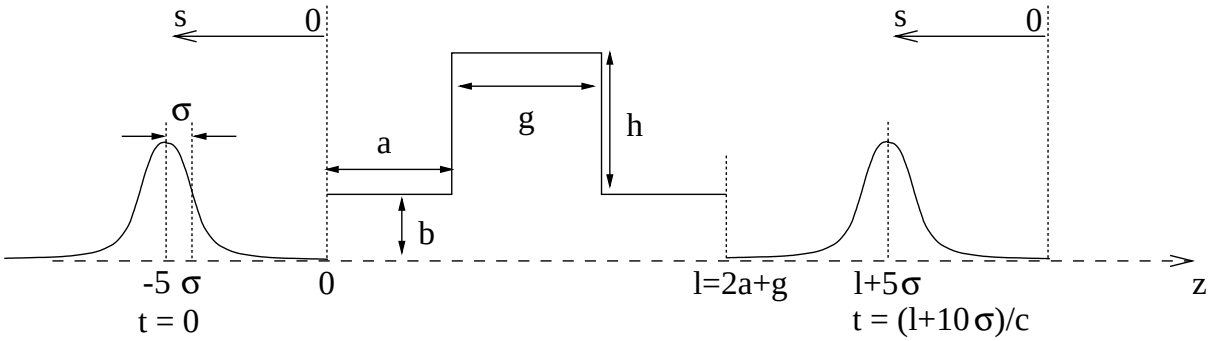

Figure 3: Definition of axial symmetric pillbox. The sketch also shows the bunch charge distribution, and the z and s coordinates, at two different times t. The bunch moves from left to right.

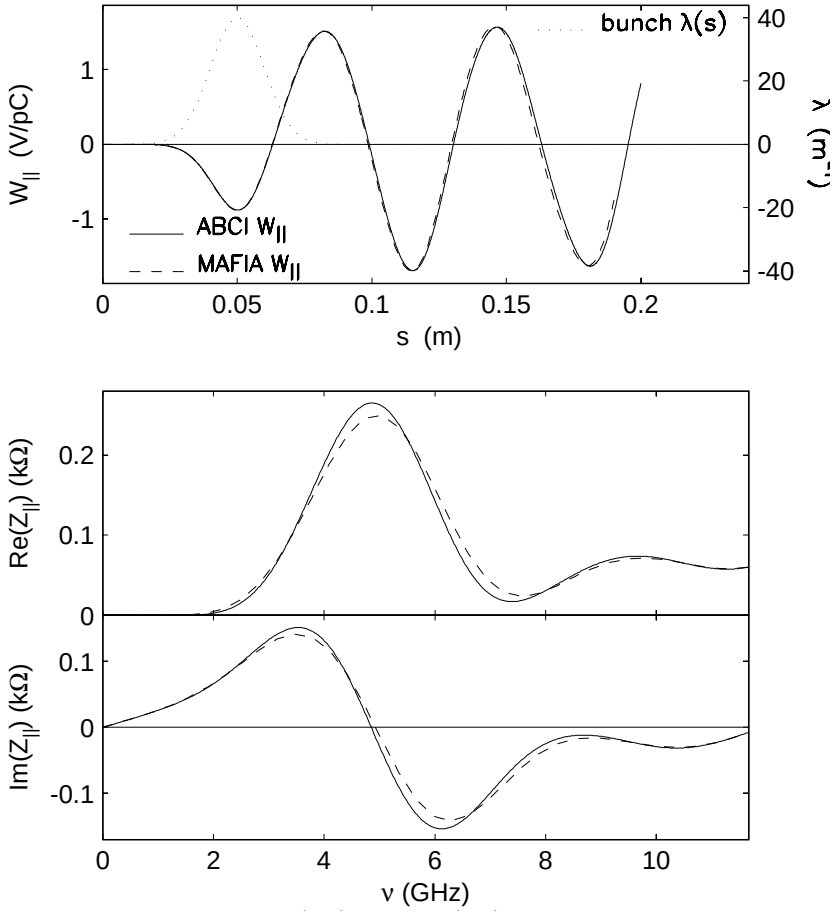

Figure 4: Comparison of $W_\parallel$, $\mathrm{Re}(Z_\parallel)$ and $\mathrm{Im}(Z_\parallel)$ obtained for a pillbox cavity from ABCI (solid curves) and MAFIA (dashed curves).

We performed a number of simulations with ABCI and MAFIA, in which we varied the mesh step size dz*, the cut-off parameter $s_{\mathrm{cut-off}}$, and the bunch length σ. From these calculations we determined the requirements $s_{\mathrm{cut-off}} \geq 20\sigma$ and $dz \leq 1$ mm. When these requirements are

*The transverse (or radial) step size was set equal to the longitudinal step size.

fulfilled, the extracted impedance slope is independent of the bunch length, as it should be. The value obtained $[d\mathrm{Im}(Z_\parallel)/dn]_{n=0} \simeq 0.28$ mΩ is in reasonable agreement with the expected value.

We further checked that the same results can be obtained with the full 3D solution of MAFIA's T3 solver with the same mesh size and $s_{\mathrm{cut-off}}$. Figure 4 shows the results obtained for the above pillbox cavity with MAFIA and ABCI. Again, good agreement is obtained.

4 Results for VELO corrugations

After performing the various checks mentioned in the previous section, we calculated with MAFIA's T3 solver the wake potential for a section of the corrugated structure shown in Fig. 2. The model consists essentially of a central section with a given number of identical (and longitudinally adjacent) corrugations. Opposite halves are separated by a 1 mm gap (thus, simulating the VELO detector in the 'closed' position) and staggered along the beam axis by half a corrugation. The corrugated section is connected at its ends to short cylindrical beam pipes of Ø12 mm (the MAFIA-T3 boundary condition at the entrance and exit of the model is 'waveguide'). Figure 5 shows a cross-section view at different lateral positions (x) for the case with two corrugations. The top sketch shows the structure at $25 < x < 100$ mm. The bottom one shows the cross-section at $x = 0$ mm, *i.e.* in the plane containing the beam axis. For changing the cavity length ℓ, only the parameter W on the figure was modified.

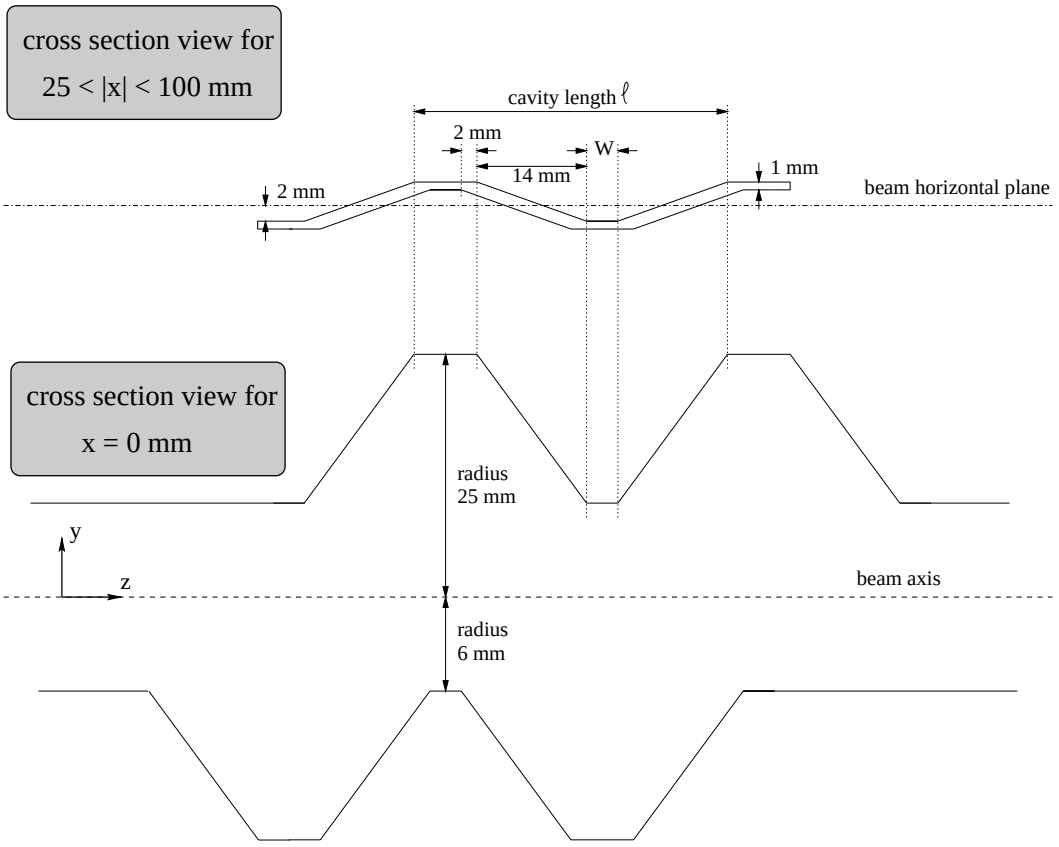

Figure 5: Definition of corrugated structure simulated with MAFIA.

The $[d\mathrm{Im}(Z_\parallel)/dn]_{n=0}$ results are shown in the left plot of Fig. 6 as a funtion of the cut-off value of s and for different numbers of cavities, cavity lengths and/or bunch lengths. The figure shows clearly that the $[d\mathrm{Im}(Z_\parallel)/dn]_{n=0}$ values have converged when $s_{\mathrm{cut-off}} \simeq 20\sigma$. Calculations were

carried out for 1, 3, 4 and 5 cavities of length $\ell = 4$ cm and with fixed $\sigma = 1$ cm (solid curves). For the case with 4 cavities, two more simulations were done with $\sigma = 5$ and 7.5 cm (long-dashed and dot-dashed curves, resp.). For $\sigma = 7.5$ cm the simulation was truncated at $s_{\rm cut-off} = 16\sigma$, but the value of $[d\mathrm{Im}(Z_\parallel)/dn]_{n=0}$ seems to converge to the same value as for $\sigma = 5$ and 1 cm. The dependence of $[d\mathrm{Im}(Z_\parallel)/dn]_{n=0}$ on the number of cavities and on the bunch length is shown on the right plot. As expected, the calculated $[d\mathrm{Im}(Z_\parallel)/dn]_{n=0}$ does not depend on σ, while it scales linearly with the number of cavities (to a good approximation).

Furthermore, for the case with a single cavity (and $\sigma = 1$ cm), additionnal calculations were carried out for a cavity length of $\ell = 6$ and 8 cm (dotted and dashed curves). The impedance slope seems to quickly saturate when increasing the cavity length.

Using these results we estimate the value $[d\mathrm{Im}(Z_\parallel)/dn]^{\rm tot}_{n=0}$ for the complete structure shown in Fig. 2 to be of the order of

$$\left.\frac{d\mathrm{Im}(Z_\parallel)}{dn}\right|^{\rm tot}_{n=0} \simeq 17 \times \left.\frac{d\mathrm{Im}(Z_\parallel)}{dn}\right|^{\ell=4\,\rm cm}_{n=0} + 9 \times \left.\frac{d\mathrm{Im}(Z_\parallel)}{dn}\right|^{\ell=8\,\rm cm}_{n=0} \simeq 5.5\ \mathrm{m\Omega}\ . \tag{4}$$

In comparison, the LHC shielded bellows and monitor tanks contribute about 120 mΩ to the effective impedance budget [12].

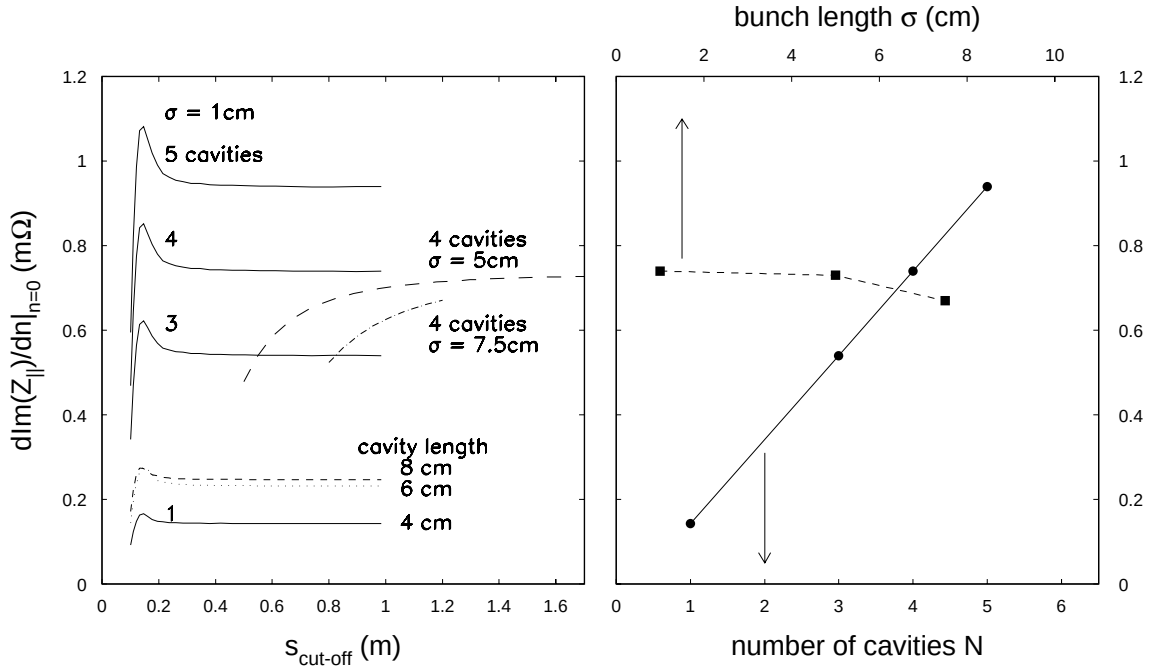

Figure 6: The left graph shows the $[d\mathrm{Im}(Z_\parallel)/dn]_{n=0}$ values obtained with the MAFIA T3 solver as a function of the cut-off value applied for the variable s to calculate the impedance from the wake function. The calculation was performed for $N = 1$, 3, 4 and 5 cavities in the model, each of 4 cm length, and with $\sigma = 1$ cm. For the case $N = 1$ the simulation was repeated for a cavity length of 6 and 8 cm. For the case $N = 4$ the simulation was repeated for $\sigma = 5$ and 7.5 cm. The right plot shows the dependence of $[d\mathrm{Im}(Z_\parallel)/dn]_{n=0}$ on N and σ, when estimating $[d\mathrm{Im}(Z_\parallel)/dn]_{n=0}$ at the highest available $s_{\rm cut-off}$.

5 Conclusions and Outlook

We performed a set of computer simulations (using the MAFIA package) to estimate the low-frequency slope of the longitudinal impedance of the LHCb VELO baseline design with the

detectors in the closed position. From these studies we expect $[d\mathrm{Im}(Z_{\|})/dn]_{n=0} \lesssim 5.5$ mΩ. Further studies will be carried out for the detectors in the open position and measurements on a one-to-one scale mock-up will be performed at NIKHEF.

Acknowledgements

We are grateful to Daniel Brandt and Lucien Vos (from CERN SL/AP) for their comments and suggestions.

References

[1] *"Mechanical Design of the LHCb Vertex Locator: Baseline Solution"*, M. Doets *et al.*, LHCb note LHCb-2001-083.

[2] *"Aperture requirements around interaction IP8"*, G. von Holtey, LHCb note LHCb-97-002.

[3] LHCb Technical Proposal, CERN/LHCC 98-4 (1998).

[4] *"A first study of wake fields in the LHCb vertex detector"* N. van Bakel, J.F.J. van den Brand, M. Ferro-Luzzi, LHCb note LHCb-99-041.

[5] *"Wake fields in the LHCb vertex detector: strip shielding"*, N.A. van Bakel, J.F.J. van den Brand, M. Ferro-Luzzi, LHCb note LHCb-99-043.

[6] *"Wake fields in the LHCb vertex detector : alternative designs for the wake field suppressor"*, N.A. van Bakel, J.F.J. van den Brand, M. Ferro-Luzzi, LHCb note LHCb-99-044.

[7] MAFIA Collaboration, CST GmbH, Lautschlagerstr 38, 64289 Darmstadt.

[8] Y.H. Chin, User's Guide for ABCI Version 8.7, CERN SL/94-02 (AP).

[9] *"Is a longitudinal feedback system required for LHC ?"*, D. Boussard, D. Brandt and L. Vos, LHC Project Note 205 (1999).

[10] See e.g. in *"Impedances and Wakes in High-Energy Particle Accelerators"*, B.W. Zotter and S.A. Kheifets, World Scientific (1998), ISBN 9810226268.

[11] *"Power Losses in Enlarged Experimental Chambers of the LHC"*, L. Vos, LHC Project Note (to be published).

[12] *" Single-Beam Collective Effects in the LHC"*, F. Ruggiero, LHC Note 313 (CERN SL/95-09 AP).